AD

Award Number: W81XWH-11-1-0441

TITLE: Role of Protein Kinase C Epsilon in Prostate Cancer and Metastasis

PRINCIPAL INVESTIGATOR: ALVARO GUTIERREZ UZQUIZA

CONTRACTING ORGANIZATION: University of Pennsylvania,
Philadelphia, PA 19104-6084

REPORT DATE: August 2013

TYPE OF REPORT: ANNUAL SUMMARY

PREPARED FOR: U.S. Army Medical Research and Materiel Command
Fort Detrick, Maryland 21702-5012

REPORT DOCUMENTATION PAGE

Form Approved
OMB No. 0704-0188

1. REPORT DATE	2. REPORT TYPE	3. DATES COVERED
August 2013	**Annual Summary**	**1 June 2011 - 31 July 2013**

4. TITLE AND SUBTITLE

"Role of Protein Kinase C Epsilon in Prostate Cancer and Metastasis"

5a. CONTRACT NUMBER
W81XWH-11-1-0441

5b. GRANT NUMBER
W81XWH-11-1-0441

5c. PROGRAM ELEMENT NUMBER

6. AUTHOR(S) 6. AUTHOR(S)
ALVARO GUTIERREZ UZQUIZA

E-Mail: alvarog@mail.med.upenn.edu

5d. PROJECT NUMBER

5e. TASK NUMBER

5f. WORK UNIT NUMBER

7. PERFORMING ORGANIZATION NAME(S) AND ADDRESS(ES)

University of Pennsylvania Department of Pharmacology
Philadelphia, PA 19104-6084

8. PERFORMING ORGANIZATION REPORT NUMBER

9. SPONSORING / MONITORING AGENCY NAME(S) AND ADDRESS(ES)
U.S. Army Medical Research and Materiel Command

Fort Detrick, Maryland 21702-5012

10. SPONSOR/MONITOR'S ACRONYM(S)

11. SPONSOR/MONITOR'S REPORT NUMBER(S)

12. DISTRIBUTION / AVAILABILITY STATEMENT
Approved for Public Release; Distribution Unlimited

13. SUPPLEMENTARY NOTES

14. ABSTRACT

The altered balance in the expression of PKC isozymes is a distinguished feature of cancer. One of the most notable alterations in epithelial cancers is the upregulation of PKCε. This kinase has emerged as a potential oncogene and tumor biomarker, however, little is known regarding a potential causality between its upregulation and cancer development. In this research we wished to understand the role played by PKCε in prostate cancer cells and establishes the proof of principle of PKCε inhibition as a putative therapeutic strategy. We already found that PKCε inhibition decreases size of tumor generated by PC3-ML cells in athymic/balb-c mice. Therefore, during this second year we have focus in the study of the metastasic properties of PKCε. Using an RNAi approach we found that PKCε depletion markedly impaired the ability of PC3-ML metastasize in bone marrow of athymic/balb-c mice. In addition we found that this kinase is relevant in attachment, MMPs activity, cytokines expression, and anchorage-dependent and anchorage- independent growth of PC3-ML cells. Moreover, we have determined that pharmacological inhibition of PKCε significantly reduced invasiveness phenotype of PC3-ML. In summary, our results argue for a role of PKCε in prostate cancer development and metastasis, highlighting its potential as a therapeutic target.

15. SUBJECT TERMS
PKCepsilon, Prostate, Cancer development, Metastasis.

16. SECURITY CLASSIFICATION OF:			17. LIMITATION OF ABSTRACT	18. NUMBER OF PAGES	19a. NAME OF RESPONSIBLE PERSON
a. REPORT	b. ABSTRACT	c. THIS PAGE			USAMRMC
U	U	U	UU	27	19b. TELEPHONE NUMBER *(include area code)*

TABLE OF CONTENTS

INTRODUCTION

The main goal of our research supported by DOD is to elucidate the mechanisms by which protein kinase C (PKC) epsilon is implicated in tumorigenesis or metastatic events in prostate cancer. The PKC family comprises 10 different isozymes, which have been classified into 3 groups: "classical" or calcium dependent PKCs (cPKCs α, βI, βII, and γ), "novel" or calcium-independent (nPKCs δ, ε, η, and θ), and "atypical" (aPKCs ζ and λ/ι). Members of the first two groups can be activated by phorbol esters, natural compounds originally described as tumor promoters. cPKCs and nPKCs are the most prominent targets for the lipid second messenger diacylglycerol (DAG), a lipid generated mainly by phospholipase C isozymes upon activation of tyrosine kinase and G-protein-coupled receptors (GPCRs). Activation of these receptors leads to DAG generation, which triggers the translocation and activation of cPKCs and nPKCs. PKC isozymes modulate important signaling pathways that control proliferation, differentiation, survival, apoptosis, and malignant transformation. While PKC has been initially viewed as a growth-promoting kinase, it became clear particularly in the last decade that PKCs could trigger growth inhibitory or apoptotic responses as well [1], [2], [3]. Despite extensive investigations, a challenge has been to establish the relative contribution of individual PKC isozymes to cancer progression, a complex task due to the vastly different roles that PKC isozymes play and the fact that these vary according to cell type. Most prostate cancer cell lines express cPKCα, nPKCδ and nPKCε. The roles of individual isozymes in mitogenesis and survival of prostate cancer cells are still a subject of debate.

Using pharmacological and molecular approaches, our laboratory established an essential role for PKCδ and PKCα in prostate cancer cell apoptosis. However, one of the most relevant and yet poorly understood member of the PKC family is *PKCε*. This kinase has been shown to act as a dominant oncogene in different cellular models [4], [5], [6], [7] and it has been implicated in neoplastic transformation and progression to a metastatic stage in NIH 3T3 fibroblast [4], [8]. PKCε is highly overexpressed in human prostate cancer. Nearly 100% of human prostate tumors overexpress PKCε, particularly advanced metastatic tumors. Evidence linked PKCε to Akt and survival in various cancer cell types [9], [10]. In prostate cancer cells PKCε functionally interacts with Bax and Akt to promote survival [11], activates the Stat3 pathway [12], and is implicated in the transition to androgen independence. Verma's group has recently demonstrated that genetic deletion of PKCε in TRAMP mice down-regulates prostatic Stat3 activation and Stat3-regulated gene expressions and inhibits prostate cancer development and metastasis [13]. A study from our lab found that PKCε promotes survival in prostate cancer cells by modulating Bad phosphorylation and the secretion of pro-apoptotic death factors [14]. In addition, using a transgenic mouse model our lab established that overexpression of PKCε in the prostate confers pre-neoplastic lesions and cooperates with Pten deficiency.

The main goal of our research is to understand the role played by PKCε and determined if PKCε inhibition is a putative therapeutic strategy.

BODY

1. Generation and characterization of PKCε-depleted cells in prostate cancer cell lines

As we have reported before we successfully established cultures of PKCε-depleted cells in the following prostate cancer cellular models: PC3, PC3-ML and DU-145. During this second year we have been working mainly with two of the cell lines already established: PC3-ML and RWPE-1. Silencing was achieved by means of infections with shRNA lentiviruses. Selection was performed for at least 3 weeks in presence of puromycin (0.3 μg/ml). Cultures were made with 5 different shRNA target sequences: #844, #845, #846, #847, #848 (MISSION shRNA Lentiviral Transduction particles, #SHCLNV Clone ID TRCN844/845/846/847/848; Sigma, St Louis, MO, USA) and the highest PKCε depletion was achieved in cells infected with sequences number #844 and #848 in all prostate cancer cells used. MISSION non-target shRNA Lentiviral Transduction particles (Sigma, SHC0016V) were used as control (NTC). Unfortunately, partial recovery of PKCε expression was detected in some of the cell lines forcing us to re-generate PKCε-depleted cells.

We decided to study the impact of PKCε depletion in PC3-ML cells in survival and proliferation pathways. Using these cell lines we could determine that PKCε-depleted cells displayed a significant reduction in levels of activated Akt, p38MAPK, Erk, and Jak/Stat pathways in PC3-ML in response to EGF stimulation. As we expected, PKCε-depleted cells have a substantial decrease of levels of activation in survival pathways after EGF stimulation or even, as Stat-1, in basal conditions (Fig. 1a).

We also overexpressed PKCε in RWPE-1 cells, a model used as "normal" non-transformed epithelial prostate cells using (ViraPower lentiviruses containing a Human PKCε construct cloned into pLenti6/V5-DEST). Selection was made for at least 3 weeks in the presence of blasticidin (0.3 μg/ml). High levels of PKCε were detected in these cells (RWPE-1-PKCε) by Western blot (Fig. 1e, right panel).

2. PKCε-deficient prostate cancer cells have impaired anchorage-dependent and anchorage-independent growth

Cell anchorage to substratum reflects the interaction of ECM with integrins and cadherins and is strongly linked with specific events such as the expression of cyclins and cell cycle progression. Several reports in the literature have established a role for PKCε in cell cycle progression [15], [16]. We speculate that silencing PKCε could have an impact on anchorage-dependent/independent growth and proliferation. As fig. 1d shows, cell proliferation was significantly reduced at 48 h in the two cell lines, where PKCε was stably depleted. As expected, PKCε overexpression increases proliferation of RWPE-1 cells. RWPE-1-PKCε display high proliferative rates compared to control cells, as determined by Crystal Violet staining (Fig. 1e, left panel).

Moreover, assays of colony formation in liquid and semisolid medium revealed that both anchorage-independent and anchorage-dependent growth were impaired in PC3-ML cells relative to control cells. Our results show that PKCε-depleted cells generated a similar number of colonies, but the size of these colonies is considerably smaller than NTC or parental (P) cells when they are grown in a semisolid medium (Fig 1b).

On the other hand, PKCε-depleted PC3-ML cells or their corresponding controls were synchronized in G0 and plated on cultured cell dishes. After 2-3 weeks, plates were stained with Methylene Blue, and number and size of colonies were determined. As shown in figure 1c, PKCε depletion caused a remarkable inhibition in the number and size of colonies, pointing out to a role of PKCε in anchorage-dependent growth in prostate cancer cell lines.

3. PKCε-deficient prostate cancer cells have impaired tumorigenic capacity

First, we carried out a preliminary assay injecting different number of PC3, DU-145 and PC3-ML cells to determine the cell concentration and kinetics of the tumor growth in our experimental conditions. We injected $1x10^6$, $3x10^6$ and $5x10^6$ or $8x10^6$ cells suspended in 100 µl of PBS in the flank of at least 3 athymic BALB/c nude mice. Tumor growth was determined every 3 days beginning at the first signs of tumor appearance. Tumors formed by PC3 and PC3-ML cell lines showed a high correlation between number of cells and size of the tumor. We could not establish a solid correlation with DU-145 cells, and therefore we focused on the other two cell lines (data not shown).

Next, we injected 4 x 10^6 PKCε-depleted PC3 cells (sequences #4 and #8) per animal (n=10) or the corresponding non-target control (NTC). We used a caliper to measure tumor cross-section area formed by PC3 cells every 3 days, and we did not detect any significant difference in size between tumors formed by PKCε-depleted cells or NTC cells during the duration of the study (Fig. 2a). As we reported during the first year, we injected 4 x 10^6 PC3-ML cells of PKCε-depleted lines (sequences #4 and #8) per animal (n=10) or the corresponding NTC (Fig. 2b). As a second approach, we decided to inject less number of cells: 1.2 x 10^6 PC3-ML PKCε depleted cells (sequences #4 and #8) per animal (n=10) or the corresponding NTC (Fig. 2c). We observed a marked difference in tumor size between the PKCε-depleted cells and NTC in both experiments (Fig. 2b, c and d); however, statistical analysis did not show significant differences. Therefore, we hypothesize that minor differences shown by PKCε-depleted cells could be the consequence of 1) impaired anchorage/anchorage-independent growth, 2) proliferation, 3) reduced levels of activated survival pathways and 4) induction of cell death in PKCε-depleted cells reported last year, as evidenced by a large number of TUNEL-positive cells (Fig. 2e).

The small differences detected in tumor sizes of PKCε-depleted PC3-ML and PC3-ML NTC cells have discouraged us to determine whether pharmacological inhibition of PKCε impairs the tumorigenic capacity of prostate cancer cell lines. We have decided to focus all our efforts in the specific aim 2; *i.e.* to determine if PKCε is implicated in invasion and metastasis of prostate cancer cells.

4. PKCε depletion affects invasiveness but not migration

We decided to analyze the migratory properties of PKCε in PC3-ML and RWPE-1 cells. We used a wound assay in order to determine whether PKCs play a role in the regulation of migratory properties in PC3-ML cells. The wound assay or wound-healing assay is used to study cell migration *in vitro*. Briefly, we scratch the surface of the culture vessel using a pipette tip creating a "wound" in a cell monolayer. Two micrographs were obtained at time = 0 h and 24 h later. Wound closure measurements were normalized to the maximum initial scratch area for each well. No significant differences were observed in terms of percentage of wound closed between P or NTC cells and PKCε-depleted cells (Fig. 3a, left panel). Then, we decided to evaluate if overexpression of PKCε in normal prostate cells (RWPE-1) confers a migratory phenotype. Due to the low migratory ability of this cell line we induced cell migration by EGF stimulation. We could not detect significant differences in percentage of wound closed in RWPE-1 or RWPE-1-PKCε cells after 24 h with or without EGF stimulation (Fig. 3a, righ panel).

To further establish the requirement of PKCε for cell motility we carried out migration assays in PC3-ML cells using Boyden chambers (Fig. 3b). P PC3-ML, PKCε-depleted PC3-ML cells (sequences #4 and #8) or NTC cells (2 x 10^4) were seeded in the upper compartment of the Boyden chamber, and FBS was used as chemoattractant. We used 12 μm polycarbonate membrane to separate the upper and lower chambers. PKCε depletion slightly decreased the migratory properties of PC3-ML cells. In addition, we examined whether PKCε overexpression in RWPE-1 cells confers a migratory phenotype. Similarly, RWPE-1 or RWPE-1-PKCε cells (2 x 10^4) were seeded in Boyden chamber, with EGF and pituitary bovine extract as chemoattractant. 12 and 8 μm polycarbonate membranes were used to separate the upper and lower chambers. No migration was detected in RWPE-1 or RWPE-1-PKCε cells after 24 h (data not shown).

Cell type-specific associations between PKCs signaling and small Rho GTPases family have been reported. Rac1, a member of the Rho family, has been widely implicated in cytoskeleton rearrangements and cell migration, and play important roles in tumorigenesis and metastasis [17]. Therefore, we examined the role of PKCε in Rac1 activity in PC3-ML. Briefly, Parental PC3-ML (P), PKCε-depleted PC3-ML cells (sequences #4 and #8) or cells infected with non-target control (NTC) shRNA lentivirus were grown at low confluence with or without FBS. Cells were lysed in pull down buffer and Rac-GTP was pulled down using PBD-GST-glutathione sepharose beads. Rac-1 was detected by Western blot using an anti-Rac1 antibody. Depletion of PKCε with either #4 or #8 RNAi duplexed reduced Rac1 activation levels under serum deprivation conditions (Fig. 3c, upper panel); however, addition of EGF induced similar Rac1 activation in all PC3-ML cell lines (Fig. 3d). On the other hand, depletion of PKCε did not have any effect on Rac1 activity in cells growing with 10% FBS (Fig. 3b, bottom panel). Surprisingly, migration in serum deprivation condition was not abolished when PKCε was knocked down and therefore Rac1 activity was reduced. Although these results may implicate PKCε as a modulator of Rac1 activity we could not correlate Rac1 levels with migratory properties in the PC3-ML cell line.

Due to the highly metastatic properties of PC3-ML cells, we also evaluated the role of PKCε in invasion through Matrigel. Fig. 4a shows that PKCε depletion strongly decreased invasiveness in PC3-ML cells. To further establish the requirement of PKCε for invasiveness in PC3-ML cells, we used εV1-2, a specific inhibitor of PKCε translocation that has been widely used in cellular and animal models [18] [19]. PC3-ML P cells were incubated with either εV1-2 or the control peptide (Tat) and analyzed for changes in motility. In agreement with results observed using PKCε RNAi, pharmacological inhibition of PKCε significantly reduced the invasive phenotype of PC3-ML cells in response to FBS (Fig. 4b).

Osteoblast-conditioned medium can attract prostate cancer cells in vitro. We hypothesize that PKCε could also regulate this mechanism. To assess if PKCε is implicated in osteoblast conditioned medium chemoattraction of prostate cancer cells, we first carried out an invasion assays in PC3-ML using Boyden chambers. As previously described, 2 x 10^4 cells were seeded in Boyden chamber, and FBS or osteoblast-conditioned medium was used as chemoattractant. As fig. 4c left panel shows, osteoblast-conditioned medium induced chemotaxis and invasion of PC3-ML cells in a dose-dependent manner. PKCε depletion, which strongly decreased invasiveness in PC3-ML cells in response to FBS, does not reduce the invasion capacity of PC3-ML in response to osteoblast-conditioned (Fig. 4c, right panel).

5. PKCε depletion does not affect adhesion to matrix but impairs the viability of PC3-ML cells in a bone marrow biomimetic microenvironment

Cancer metastasis is a multistep process involving many types of cell-cell interactions, including adhesive interactions and signaling events during extravasation and establishment in a new organ. We carried out adhesion assays to assess the involvement of PKCε ECM interactions. Briefly, 10 x 10^5 parental PC3-ML (P), PKCε-depleted PC3-ML cells (sequences #4 and #8) or NTC cells were seeded over culture plates non-coated or coated with Matrigel, collagen or poly-L-lysine. After different times, cells were rinsed twice with PBS, fixed, and stained with DAPI. The number of attached cells was quantified with the ImageJ software. As shown in Figure 5a, PKCε depletion significantly impairs adhesion of PC3-ML cells to non-coated plates at 30 min. Surprisingly PKCε depletion did not affect the adhesion of PC3-ML cells to Matrigel, collagen or poly-L-lysine.

Cell-cell and cell-matrix interactions play a major role in tumor morphogenesis and cancer metastasis. Therefore it is crucial to create a model with a biomimetic microenvironment that allows us to study those interactions *in vitro*. Endothelial cells of the bone marrow and osteoblasts are thought to express selected adhesion molecules that could "capture" prostate cancer cells from the blood stream. Those factors are able to modify the invasive, survival and adherent capability of prostate cancer cells [20]. To assess if PKCε confers survival advantage in the new microenvironment, we examined the ability of the PC3-ML cells (P, PKCε siRNA duplexes #4 and #8, or NTC) to adhere and proliferate when seeded on top of a confluent layer of human osteoblast cells (MG-63). Briefly, 5 x 10^3 PC3-ML cells (P, PKCε-depleted PC3-ML or NTC) were transfected with a lentiviral-enhanced green fluorescent protein expression vector (ZsGreen, a variant of wild-type Zoanthus sp. green fluorescent protein) and were seeded over a confluent monolayer of MG-63. After different times non-attached cells were rinsed with PBS.

Three weeks later the number of PC3-ML foci was quantified. As Fig. 5b shows, P or NTC cells were able to attach and proliferate in a time-dependent manner. However, only a small number of PKCε-depleted cells were able to attach and proliferate under the new microenvironment conditions. These results suggest that PKCε may be implicated in the survival and adherent capability of prostate cancer cells in the tumor microenvironment.

6. PKCε confers prostate cancer cell resistance to loss of viability induced by absence of attachment

To gain insight into the molecular mechanisms underlying metastasis we explored the role of PKCε in tumor cell survival from detachment-induced apoptosis (*i.e.* anoikis). Briefly, $1x10^6$ PC3-ML cells (P, PKCε-depleted PC3-ML or NTC) were detached and kept in suspension for different times. PKCε knock-down led to a significant reduction in anchorage-dependent growth after long times in suspension (12 h) compared to wt or NTC PC3-ML cells, suggesting that PKCε mediates anti-anoikis events in the bloodstream. No significant differences could be detected at short times (2 h) (Fig 6). In conclusion, PKCε confers prostate cancer cell resistance to loss of viability induced by absence of attachment, which could potentially contribute to prostate cancer metastasis.

7. PKCε-depletion affects the activity of proteolytic enzymes in basal conditions

Fig. 4a and b show that PKCε-depleted PC3-ML cells essentially lost their ability to migrate through Matrigel. On the other hand, knocking down PKCε from PC3-ML cells did not affect the adhesion to Matrigel (Fig. 5a). These findings suggest that PKCε plays a critical role in the remodeling of the matrix and prompted us to investigate the expression of relevant ECM proteases and protease inhibitors. A set of experiments was carried out to evaluate the effect of PKCε depletion on the activity of MMP-2 and MMP-9. Conditioned medium (CM) from PKCε-depleted PC3-ML cells or their corresponding control cell lines were collected and MMP-2 and MMP-9 activities were determined by zymography on gelatin-impregnated gels. We detected differences in basal conditions in MMP-9 activity and in a high molecular weight MMP-complex (over 125 kda) (Fig. 7a, left panel). To further establish the requirement of PKCε for invasiveness we determined by zymography on gelatin-impregnated gels MMP-2 and MMP-9 activities of CM from PKCε overexpressed in RWPE-1 cells and its corresponding controls. As fig. 7a right panel shows, PKCε-overexpressed RWPE-1 cells showed a markedly increased in MMP-9 activity compared to RWPE-1 control cells.

As a second approach, we determined the expression of 84 genes known to be involved in metastasis using a Human Tumor Metastasis RT2 Profiler PCR array (Super Array Bioscience, Frederick, MD, USA). Interestingly, mRNA levels of Cadherin 5, IL-1β, MMP-7 and MMP-11 were down-regulated in PKCε-depleted PC3-ML cells (Fig. 7b).

8. PKCε mediates metastasic dissemination to the bone of PC3-ML prostate cancer cells

After successfully generating PKCε-knocked-down PC3-ML cell lines (Fig. 8a), cells

were infected with ZsGreen Lentivirus (which encodes a variant of wild-type Zoanthus sp. green fluorescent protein). 5 x 10^4 cells from the brightest population were inoculated in the left cardiac ventricle of athymic nude mice. Mice were sacrificed three weeks later and their organs processed for cryosectioning and histology. Animals that were inoculated with P or NTC PC3-ML cells displayed micrometastasis in the tibia and/or femur that seemed significantly reduced in number in those in mice inoculated with PKCε–depleted cells (Fig. 8b and c). Interestingly no micrometastasis were observed in mice inoculated with cells infected with sequence number #4, however we could find one micrometastasis in one of the animals injected with cells infected with sequence number #8, which showed moderate PKCε depletion (Fig. 8b and c).

In addition to histology analysis we established bone marrow cell cultures to isolate and quantify number of viable cell PC3-ML cells from bone marrow after intracardiac injection of PC3-ML cells (P, NTC or siPKCε). After three weeks bone marrows of both femurs were flushed and cultures of bone marrow cell preparations were developed. After seven days the number of green colonies was quantified. We detected a high number of green labeled-PC3-ML cells in cultures of bone marrow cell preparations from animals injected with P or NTC PC3-ML cells; however, no green-labelled cells could be detected in cultures of bone marrow cell preparations from animals injected with PKCε-depleted PC3-ML(Fig. 9a).

In addition, P or NTC PC3-ML sub-lines derived from cultures of bone marrow cell preparations were successfully isolated. The new sub-lines showed similar characteristics than original PC3-ML cells (Fig. 9b). However, more analysis should be made to fully characterize these new cell lines.

Unfortunately, a partial recovery of PKCε expression was detected in some of the cell lines forcing us to re-generate PKCε-depleted cells. The new generation of cell lines caused a delay in the experiments, which did not allow us to complete if pharmacological inhibition of PKCε inhibit the metastatic capacity of prostate cancer cells.

9. PKCε may regulate an autocrine/paracrine pathway implicated in metastasic dissemination to the bone of PC3-ML prostate cancer cells

Recently findings have demonstrated the importance of autocrine/paracrine loops in metastasic dissemination to the bone of prostate cancer cells. The Human Tumor Metastasis RT2 Profiler PCR array (Fig. 7b) and subsequent Q-PCR validations (Fig. 10a) established that mRNA levels of IL-1β were down-regulated in PKCε depleted cells. In addition, several reports showed that exogenous overexpression of IL-1β in non-metastatic cancer cells promotes their growth into large skeletal lesions in mice, whereas its knockdown significantly impairs the bone progression of PC3-ML cells. To further establish the requirement of PKCε in IL-1β pathway, we examined IL-1β mRNA levels by Q-PCR in PC3-ML cells. As fig. 10a shows IL-1β mRNA levels were significantly reduced in PKCε-depleted cells relative to control cells. Next, we decided to analyze the signaling events induced by cytokines from PC3-ML conditioned medium in osteoblast cells. Human osteoblast MG-63 cells constitutively express IL-6, which it is known to activate Stat-3, and it has been shown that IL-1β impairs IL-6-induced Jak/Stat [21]. We hypothesized that levels of IL-1β from PC3-ML CM could impair endogenous IL-6 signaling events in MG-63 cells. As we expected, we detected a reduction of Stat-3 tyrosine phosphorylation and increased ERK activation in MG-63 after stimulation with CM from P or NTC PC3-ML cells compared to MG-63 no treated or treated with CM from PKCε-depleted

cells (Fig. 10b). In conclusion, PKCε regulates an autocrine/paracrine pathway that may be implicated in metastasic dissemination to the bone of PC3-ML prostate cancer cells.

KEY RESEARCH ACOMPLISHMENTS

We successfully knocked down PKCε in DU-145, PC3 and PC3-ML cells.

We successfully overexpressed PKCε in RWPE-1 cells.

We found that PKCε causes a substantial decrease in the levels of activation of survival pathways after EGF stimulation

We found a marked induction of cell death in PKCε-depleted cells upon inoculation into nude mice.

We determined that PKCε mediates invasiveness of PC3-ML and PC3 cell lines.

We successfully demonstrated that pharmacological inhibition of PKCε impairs invasiveness of PC3-ML cells.

We found that PKCε depletion decreases the number of skeletal micrometastasis generated by PC3-ML cells in athymic/balb-c mice.

We determined that PKCε controls the expression of chemokines, MMPs and other molecules implicated in metastasis in PC3-ML cells.

We successfully isolated and started the characterization process of PC3-ML human prostatic tumor sublines from mouse skeletal metastases.

We found that PKCε is implicated in the attachment, MMPs activity, viability and anchorage-dependent and independent cell growth of PC3-ML cells.

CONCLUSION

The main conclusion from the research carried out during the second year of DOD funding is that PKCε plays a role in the metastasic capacity of prostate cancer cells. Our results suggest a main role of PKCε in prostate cancer cell metastatic dissemination. PKCε may be relevant in proliferation, adhesion, MMPs expression, anchorage-dependent and anchorage-independent cell growth. Pharmacological inhibition of PKCε could represent a potential approach for prostate cancer therapeutics. It is also conceivable that PKCε plays a role in metastasic dissemination to the bone through regulation of autocrine/paracrine pathways implicated in cell death/survival. We will continue with our studies to address the role of PKCε in the control of relevant metastasic events.

REPORTABLE OUTCOMES

The followings cells lines have been generated:

- PKCε-depleted cells in the following prostate cancer cellular models: PC3, PC3-ML and DU-145PC3 cells.
- PKCε-depleted cells ZsGreen expressing in the following prostate cancer cellular models: PC3-ML cells.
- PKCε-overexpressed in non-transformed RWPE-1prostate cells.

Conference attendance:

AACR Annual Meeting 2013. April 6-10, 2013
Washington, DC

This conference allowed me to assist to sessions with highly relevant scientific content and advance my knowledge on new technologies in the field. Attending this conference also it allowed me to network with other professionals in academy and the pharmaceutical industry.

I plan to assist to:

"Hormone-Dependent Cancers Development and Progression" meeting
July 28 - August 2, 2013
Bryant University
Smithfield, RI
Chair: Karen E. Knudsen

REFERENCES

1. Griner, E.M. and M.G. Kazanietz, Protein kinase C and other diacylglycerol effectors in cancer. Nat Rev Cancer. **7**, 281-94 (2007).
2. Newton, A.C., Protein kinase C: structural and spatial regulation by phosphorylation, cofactors, and macromolecular interactions. Chem Rev. **101**, 2353-64 (2001).
3. Parekh, D.B., W. Ziegler, and P.J. Parker, Multiple pathways control protein kinase C phosphorylation. EMBO J. **19**, 496-503 (2000).
4. Cacace, A.M., S.N. Guadagno, R.S. Krauss, D. Fabbro, and I.B. Weinstein, The epsilon isoform of protein kinase C is an oncogene when overexpressed in rat fibroblasts. Oncogene. **8**, 2095-104 (1993).
5. Cai, H., U. Smola, V. Wixler, I. Eisenmann-Tappe, M.T. Diaz-Meco, J. Moscat, et al., Role of diacylglycerol-regulated protein kinase C isotypes in growth factor activation of the Raf-1 protein kinase. Mol Cell Biol. **17**, 732-41 (1997).
6. Perletti, G.P., M. Folini, H.C. Lin, H. Mischak, F. Piccinini, and A.H. Tashjian, Jr., Overexpression of protein kinase C epsilon is oncogenic in rat colonic epithelial cells. Oncogene. **12**, 847-54 (1996).
7. Caino, M.C., C. Lopez-Haber, J. Kim, D. Mochly-Rosen, and M.G. Kazanietz, Proteins kinase Cvarepsilon is required for non-small cell lung carcinoma growth and regulates the expression of apoptotic genes. Oncogene. **31**, 2593-600 (2012).
8. Tachado, S.D., M.W. Mayhew, G.G. Wescott, T.L. Foreman, C.D. Goodwin, M.A. McJilton, et al., Regulation of tumor invasion and metastasis in protein kinase C epsilon-transformed NIH3T3 fibroblasts. J Cell Biochem. **85**, 785-97 (2002).
9. Lu, D., J. Huang, and A. Basu, Protein kinase Cepsilon activates protein kinase B/Akt via DNA-PK to protect against tumor necrosis factor-alpha-induced cell death. J Biol Chem. **281**, 22799-807 (2006).
10. Okhrimenko, H., W. Lu, C. Xiang, N. Hamburger, G. Kazimirsky, and C. Brodie, Protein kinase C-epsilon regulates the apoptosis and survival of glioma cells. Cancer Res. **65**, 7301-9 (2005).
11. McJilton, M.A., C. Van Sikes, G.G. Wescott, D. Wu, T.L. Foreman, C.W. Gregory, et al., Protein kinase Cepsilon interacts with Bax and promotes survival of human prostate cancer cells. Oncogene. **22**, 7958-68 (2003).
12. Aziz, M.H., H.T. Manoharan, D.R. Church, N.E. Dreckschmidt, W. Zhong, T.D. Oberley, et al., Protein kinase Cepsilon interacts with signal transducers and activators of transcription 3 (Stat3), phosphorylates Stat3Ser727, and regulates its constitutive activation in prostate cancer. Cancer Res. **67**, 8828-38 (2007).
13. Hafeez, B.B., W. Zhong, J. Weichert, N.E. Dreckschmidt, M.S. Jamal, and A.K. Verma, Genetic ablation of PKC epsilon inhibits prostate cancer development and metastasis in transgenic mouse model of prostate adenocarcinoma. Cancer Res. **71**, 2318-27 (2011).
14. Meshki, J., M.C. Caino, V.A. von Burstin, E. Griner, and M.G. Kazanietz, Regulation of prostate cancer cell survival by protein kinase Cepsilon involves bad phosphorylation and modulation of the TNFalpha/JNK pathway. J Biol Chem. **285**, 26033-40 (2010).
15. Wu, D., T.L. Foreman, C.W. Gregory, M.A. McJilton, G.G. Wescott, O.H. Ford, et al., Protein kinase cepsilon has the potential to advance the recurrence of human prostate cancer. Cancer Res. **62**, 2423-9 (2002).

16. Soh, J.W. and I.B. Weinstein, Roles of specific isoforms of protein kinase C in the transcriptional control of cyclin D1 and related genes. J Biol Chem. **278**, 34709-16 (2003).
17. Schmitz, A.A., E.E. Govek, B. Bottner, and L. Van Aelst, Rho GTPases: signaling, migration, and invasion. Exp Cell Res. **261**, 1-12 (2000).
18. Budas, G.R. and D. Mochly-Rosen, Mitochondrial protein kinase Cepsilon (PKCepsilon): emerging role in cardiac protection from ischaemic damage. Biochem Soc Trans. **35**, 1052-4 (2007).
19. Caino, M.C., C. Lopez-Haber, J.L. Kissil, and M.G. Kazanietz, Non-small cell lung carcinoma cell motility, rac activation and metastatic dissemination are mediated by protein kinase C epsilon. PLoS One. **7**, e31714 (2012).
20. Millimaggi, D., C. Festuccia, A. Angelucci, S. D'Ascenzo, N. Rucci, S. Flati, et al., Osteoblast-conditioned media stimulate membrane vesicle shedding in prostate cancer cells. Int J Oncol. **28**, 909-14 (2006).
21. Radtke, S., S. Wuller, X.P. Yang, B.E. Lippok, B. Mutze, C. Mais, et al., Cross-regulation of cytokine signalling: pro-inflammatory cytokines restrict IL-6 signalling through receptor internalisation and degradation. J Cell Sci. **123**, 947-59 (2010).

APPENDICES

FIGURE LEGENDS:

Figure 1: Characterization of PKCε depleted prostate cancer cell lines: (a) PC3-ML cell parental (P), were infected with non-target shRNA (NTC) or shRNA lentiviruses for PKCε (sequences #4 and #8). Levels of PKCε, P-Stat1-S727, P-Akt, PERKs, and P-p38 were analyzed by western blot using anti PKCε, P-Stat1-S727, P-Akt, P-ERKs, and P-p38 antibodies (Santa Cruz, Santa Cruz, CA,# sc-214, Cell signaling, Danvers, MA, #9177, #9271, #9101, and #9211). Vinculin (Sigma-Aldrich, St Louis , 0MO, # V-9131) was used as loading control. (b) To evaluate anchorage-independent growth, 3×10^3 PC3-ML (P, NTC, #4 and #8) cells were plated in 0.35% agar over a 0.5% agar layer. After 10 days, the number of colonies was quantified by MTT assay (a colorimetric cell viability assay). (c) PC3-ML (P, NTC, #4, and #8) at 80% confluency were synchronized and plated in 100 mm plates (100 cells/plate). Medium was replaced twice a week, and after 15 days colonies were stained with 0.7% methylene blue in 50% ethanol. (d) PC3-ML wt, cells at 80% confluency were synchronized to G0 and seeded in medium supplemented with 10% serum. After different times the number of cells attached was quantified by MTT assay. (e) RWPE-1 cells were infected with ViraPower lentiviruses containing a Human PKCε construct cloned into pLenti6/V5-DEST. Right panel; Expression of PKCε was analyzed by western blot using an anti PKCε antibody (Santa Cruz # sc-214). Vinculin was used as control. Left panel, RWPE-1 and RWPE-1-PKCε cells at 80% confluency were synchronized to G0 and seeded in medium supplemented with 10% serum. After 48 h the attached (=viable) cells were quantified by Crystal Violet staining.

Figure 2: PKCε is required for PC3-ML tumor growth in athymic nude mice. (a, b and c) PC3 and PC3-ML (P, NTC, #4, and #8) at 80% confluency were resuspended in PBS, and then 0.1 ml containing the number of cells indicated were injected subcutaneously into the flank of male athymic nude-Foxn1nu mice (Harlan Laboratories, Indianapolis, IN, USA). The width and length of tumors were measured with a caliper at different times, and tumor cross section area was calculated as $Vol = \pi \times w/2 \times L/2$. Data are expressed as mean ± S.D. (n=10). (d) Representative pictures of mice showing tumors generated by NTC (red arrow) or PKCε-depleted cells (blue arrow) after 24 days. (e) 15 days post inoculation, tumors were removed and processed for immunohistochemistry (TUNEL).

Figure 3: PKCε depletion affects Rac-1 activity but not migration (a) Confluent monolayers of PC3-ML (P, NTC, #4 and #8) or RWPE-1 and RWPE-1-PKCε overexpressed (RWPE-PKC) cells were scraped. Closure of wounds was recorded at 24 h post-treatment. Experiments were carried out in triplicates. Results are expressed as percentage of the closure, and expressed as mean ± S.E.M. (n = 3). (b) PC3-ML (P, NTC, #4, and #8) at 80% confluency were synchronized and 2 $x10^5$ were seeded in the upper compartment of Boyden chamber, and FBS was used as chemoattractant; 12 μm polycarbonate membrane were used to separate both chambers. (c) PC3-ML (P, NTC, #4, and #8) cells were incubated either in presence of serum or serum starved for 24 h and Rac-GTP levels were determined using a pull-down assay. A representative experiment is shown. (d) PC3-ML cells were serum starved for 24 h and treated with EGF (100 ng/ml) for 5 min, and Rac-GTP leves were determined using a pull-down assay. A representative experiment

is shown.

Figure 4: PKCε is required for migration and invasion in PC3-ML cells. PC3-ML cells (P, NTC, #4, and #8) at 80% confluency were synchronized and 2 x 10^5 were seeded in the upper compartment of Boyden chamber. 12 μm polycarbonate membrane coated with Matrigel was used to separate both chambers. Cells that invaded were stained with toluidine blue. The number of cells was counted and normalized to P (represented in graphs). Data are expressed as mean ± S.D. (n = 3). (a) Absence or 10% FBS were used as chemoattractants. (b) Absence or 10% FBS were used as chemoattractants for P cells in presence of either 1 μM εV1-2 (specific PKCε inhibitor) or control Tat (1 μM). (c) Left panel: Serial dilutions of osteoblast-conditioned medium (CM) were used as chemoattractants. Right panel: No FBS, CM or 10% FBS as chemoattractants.

Figure 5: PKCε depletion does not affect adhesion to ECM but impairs viability of PC3-ML in a Bone Marrow biomimetic microenvironment. (a) 1 x 10^5 PC3-ML (P, NTC, #4, and #8) were seeded by triplicates over culture plates non-coated or coated with matrigel, collagen or Poly-L-Lysine. At different times, cells were rinsed twice with PBS, fixed and stained with DAPI. The amount of cells was counted and normalized to P. (b) left panel; 5 x 10^3 cells PC3-ML (P, NTC, #4 and #8) were seeded over a human osteoblast monolayer. At different times, cells were rinsed twice with PBS, fixed and stained with DAPI. The amount of green foci was counted and normalized to P. Right panel: Representative pictures of green foci; Bright field (BF), Blue Channel (BC).

Figure 6: PKCε confers prostate cancer cell resistance to loss of viability induced by absence of attachment. Upper panels: PC3-ML (P, NTC, #4, and #8) at 80% confluency were synchronized kept in suspension for 2 or 12 hours and plated in 100 mm plates (100 cells/plate). Medium was replaced twice a week, and after 15 days colonies were stained with 0.7% methylene blue in 50% ethanol. Bottom panels: Expression of PKCε was analyzed by western blot using an anti PKCε antibody (Santa Cruz # sc-214).

Figure 7: PKCε-depletion affects activity of proteolytic enzymes in basal conditions: (a) left panel: Equal amount of volumes of conditioned medium (CM) of PC3-ML (P, NTC, #4, and #8) or MG-63 (used as positive control; C+) at 80% confluency were loaded in gelatin-impregnated gel (Invitrogen, Grand Island, NY; # EC6175BOX) and subjected to a gelatin zymography experiment following the manufacturer's protocol. Right panel: assessment of MMP-2 and MMP-9 activity using gelatin zymography in RWPE-1 or RWPE-1 PKCε overexpressed (RWPE PKC). CM of MG-63 was used as positive control (C+). (b) Analysis of 84 genes known to be involved in metastasis by Human Tumor Metastasis RT2 Profiler PCR array (Super Array Bioscience, Frederick, MD, USA) was performed in control or PKCε-depleted cells. Upper panel: Heat map representation of ΔΔCt-based fold-change. Bottom panel: Tumor Metastasis PCR array layout. Fold change is represented and genes up- or down- regulated more than 1.5 times are highlighted in red or green, respectively.

Figure 8: PKCε mediates metastasic dissemination to the bone of PC3-ML prostate cancer cells. Eight-week-old male athymic nude-Foxn1nu mice were inoculated with PC3-ML cells (P, NTC, #4, and #8) expressing an enhanced variant of ZsGreen through the left cardiac ventricle.

After 3 weeks, mice were euthanized, their tibiae and femora were cryosectioned, and skeletal micrometastasis were identified by fluorescence stereomicroscopy. (a) Expression of PKCε was analyzed by western blot using an anti PKCε antibody (Santa Cruz # sc-214). (b) Number of skeletal micrometastasis found. (c) Representative pictures of skeletal micrometastasis. Red arrows indicate small metastatic foci.

Figure 9: PKCε mediates metastasic dissemination of PC3-ML prostate cancer cells to the bones. Eight-week-old male athymic nude-Foxn1nu mice were inoculated with PC3-ML (P, NTC, #4, and #8) cells expressing an enhanced variant of ZsGreen through the left cardiac ventricle. After 3 weeks, mice were euthanized, their tibiae and femora were flushed and cultures of bone marrow cell preparations were developed. Briefly, both ends of bone were clipped with a scissor; after that a syringe with media was inserted into one end and bone marrow was flushed out to the other end. After 7 days, the number of green colonies was quantified. (a) Representative picture showing mouse macrophages and PC3-ML (P, NTC) cells expressing ZsGreen from bone marrow. No PKCε-depleted PC3-ML cells expressing ZsGreen were detected. (b) Left panel: PC3-ML parental (P) or PC3-ML parental cells isolated from bone marrow (P-BM) were serum starved for 24 h and treated with EGF (100 ng/ml) for 5 min. Levels of PKCε, P-Akt and P-ERKs were analyzed by western blot using anti-PKCε, P-Akt, and P-ERKs antibodies (Santa Cruz, # sc-214, Cell signaling, #9271, #9101). Vinculin (Sigma-Aldrich, St Louis MO, # V-9131) was used as loading control. Right panel: Representative pictures showing ZsGreen expression.

Figure 10: PKCε regulate expression and secretion of IL-1β in PC3-ML prostate cancer cells. (a) IL-1β and PKCε mRNA expression levels were determine by Q-PCR in PC3-ML (P, NTC, #4 and #8) (b) left panel: Human osteoblast MG-63 at 80% confluency were treated with same volume of conditioned medium (CM) from PC3-ML cells (P, NTC, #4, and #8). Levels of P-Stat-3, P-Akt and P-ERKs were analyzed by western blot using anti P-Stat-3, P-Akt and P-ERKs antibodies (Cell signaling #9134, #9271, and #9101). Vinculin (Sigma-Aldrich, # V-9131) was used as loading control. Right panel: Expression of PKCε was analyzed in PC3-ML cells by western blot using an anti PKCε antibody (Santa Cruz, # sc-214)

Figure 1

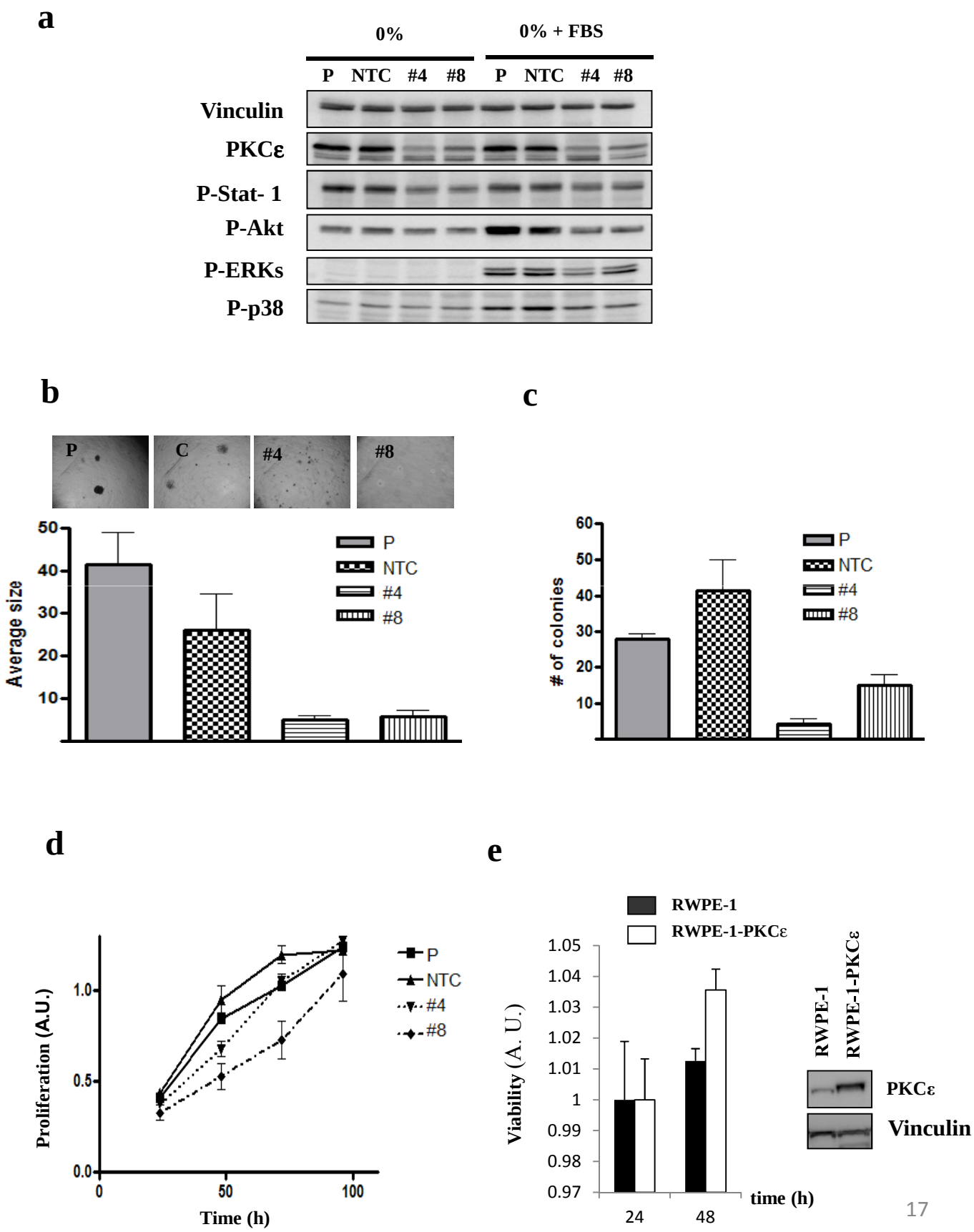
a
0%
0% + FBS
P NTC #4 #8 P NTC #4 #8
Vinculin
PKCε
P-Stat- 1
P-Akt
P-ERKs
P-p38
b
P
C
#4
#8
Average size
50
40
30
20
10
P
NTC
#4
#8
c
# of colonies
60
50
40
30
20
10
P
NTC
#4
#8
d
Proliferation (A.U.)
1.0
0.5
0.0
0
50
100
Time (h)
P
NTC
#4
#8
e
RWPE-1
RWPE-1-PKCε
Viability (A. U.)
1.05
1.04
1.03
1.02
1.01
1
0.99
0.98
0.97
24
48
time (h)
RWPE-1
RWPE-1-PKCε
PKCε
Vinculin

Figure 2

a

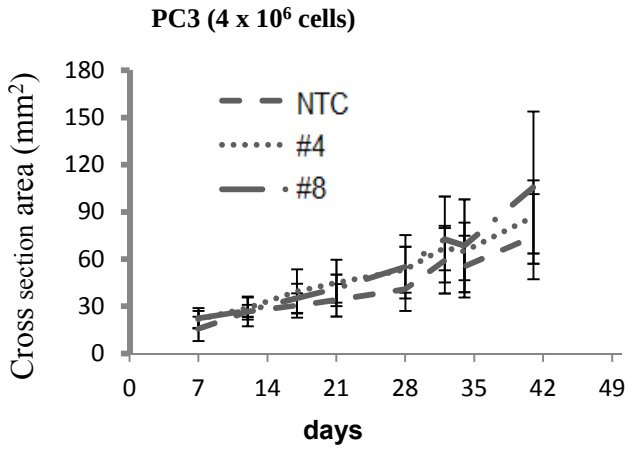

b

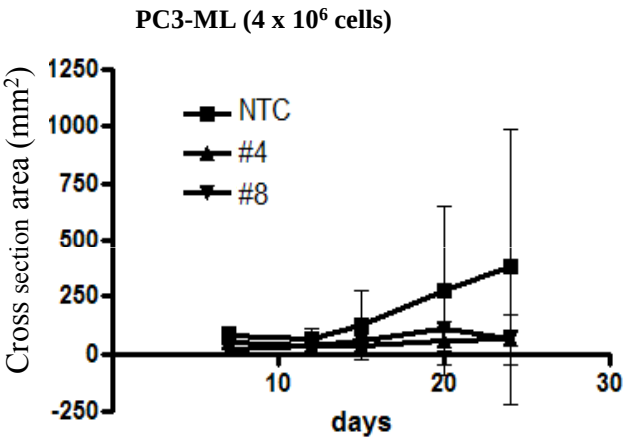

c

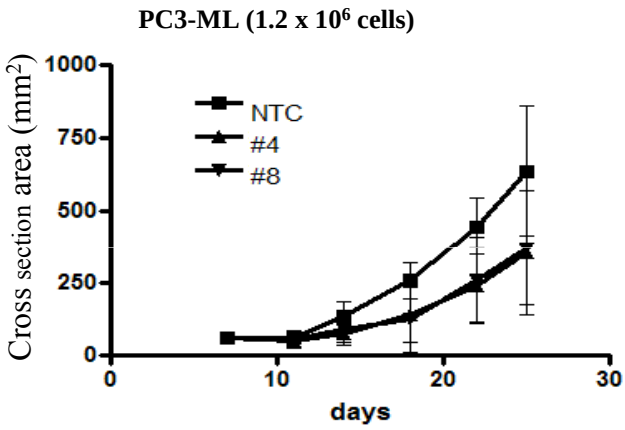

d

e

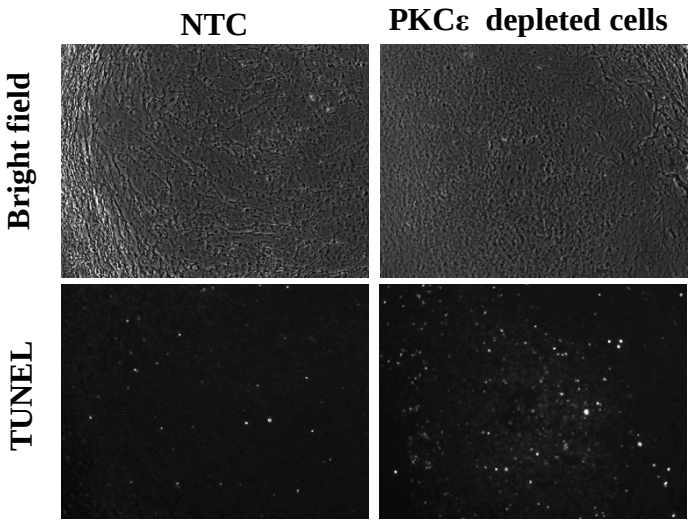

Figure 3

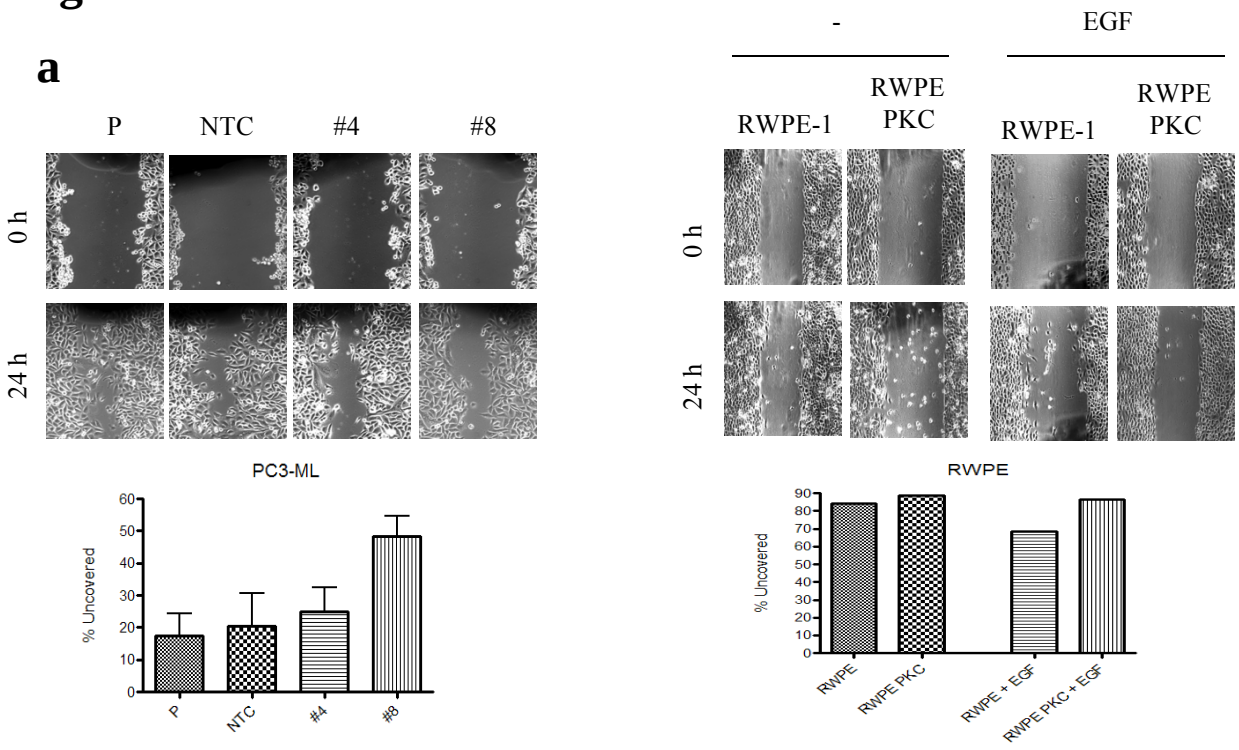
a
P
NTC
#4
#8
0 h
24 h
PC3-ML
% Uncovered
-
EGF
RWPE-1
RWPE PKC
RWPE
RWPE PKC + EGF

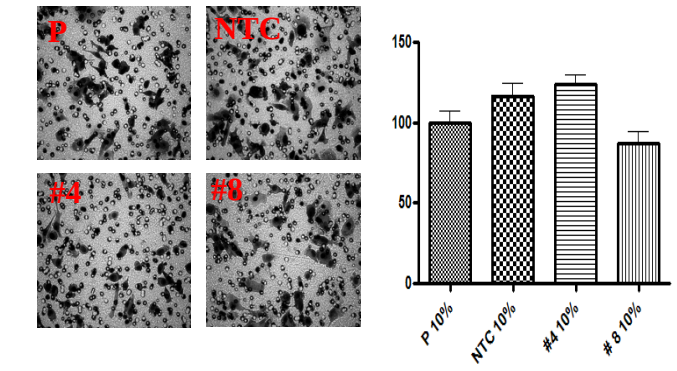
b
P
NTC
#4
#8
P 10%
NTC 10%
#4 10%
8 10%

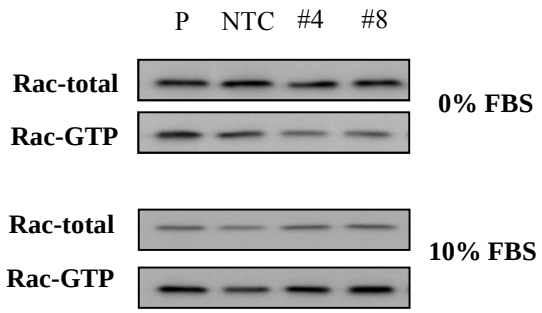
c
P
NTC
#4
#8
Rac-total
Rac-GTP
0% FBS
10% FBS

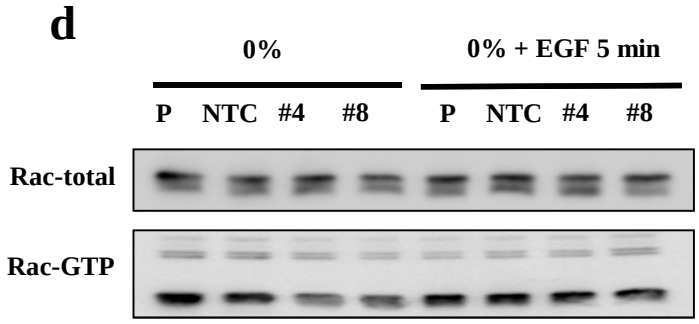
d
0%
0% + EGF 5 min
P
NTC
#4
#8
Rac-total
Rac-GTP

Figure 4

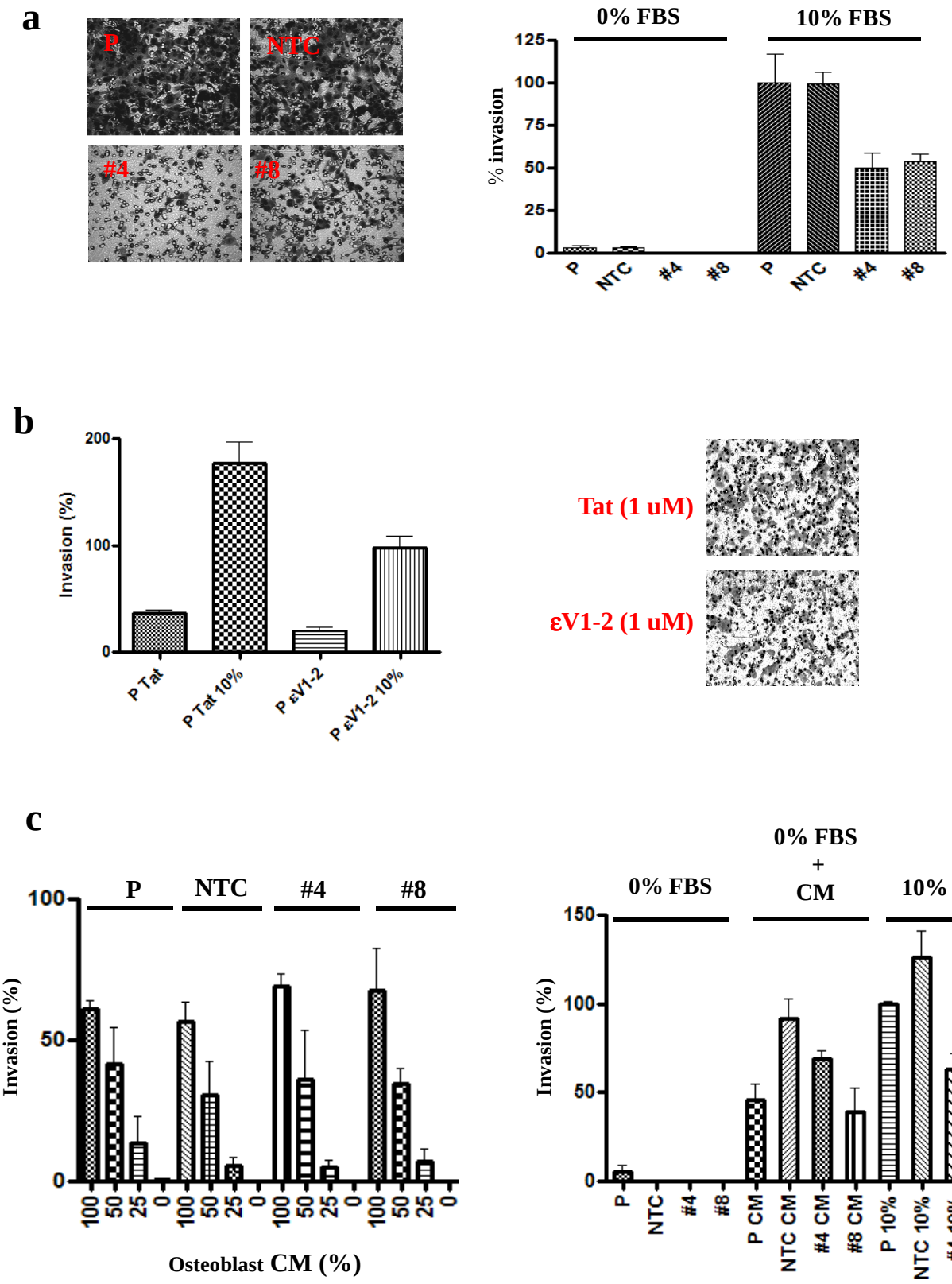
a
P
NTC
#4
#8
0% FBS
10% FBS
% invasion
125
100
75
50
25
0
P
NTC
#4
#8
P
NTC
#4
#8
b
Invasion (%)
200
100
0
P Tat
P Tat 10%
P εV1-2
P εV1-2 10%
Tat (1 uM)
εV1-2 (1 uM)
c
P
NTC
#4
#8
100
50
0
Invasion (%)
100 50 25 0 100 50 25 0 100 50 25 0 100 50 25 0
Osteoblast CM (%)
0% FBS
0% FBS + CM
10% FBS
150
100
50
0
Invasion (%)
P
NTC
#4
#8
P CM
NTC CM
#4 CM
#8 CM
P 10%
NTC 10%
#4 10%
#8 10%

Figure 5

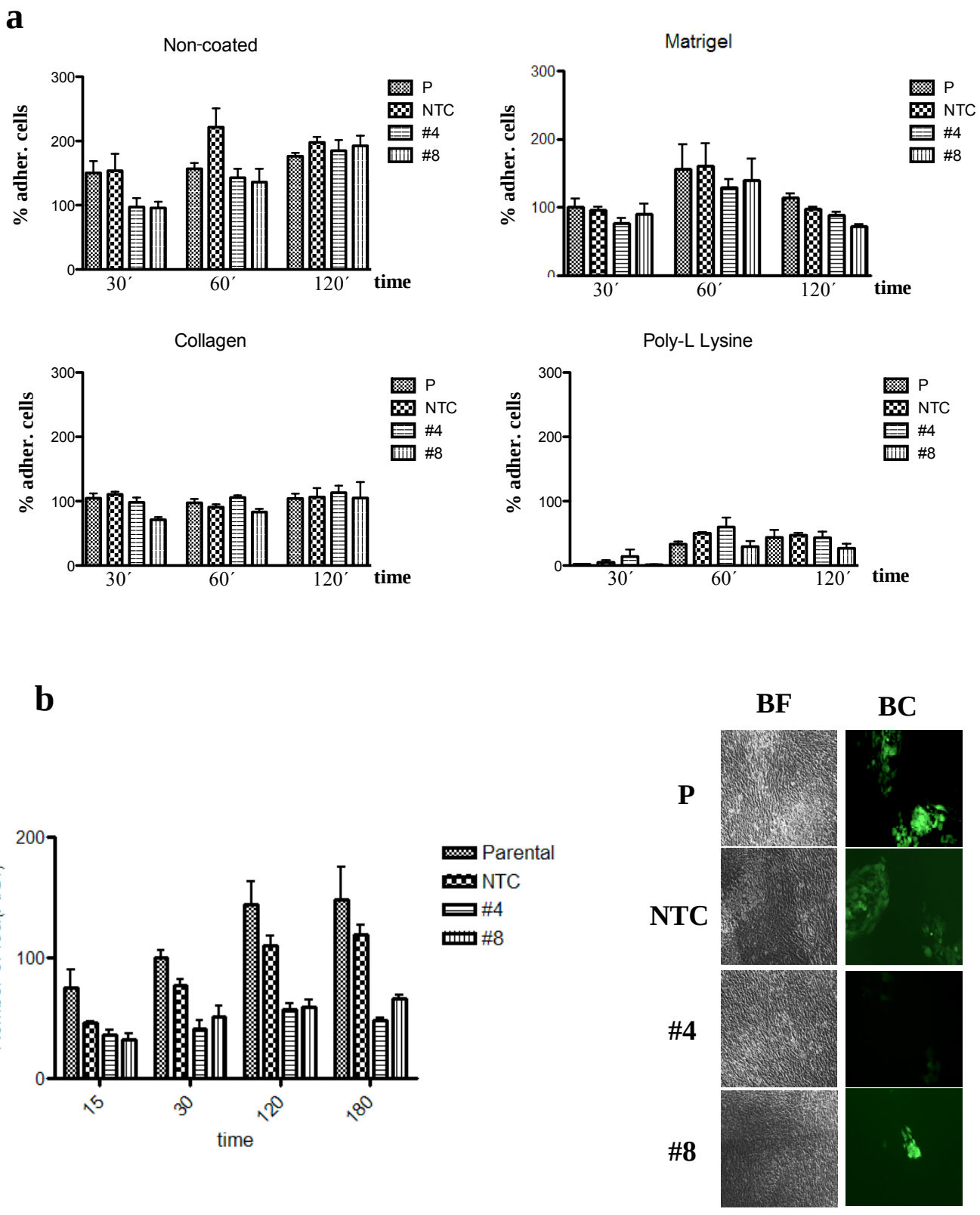
a
Non-coated
Matrigel
Collagen
Poly-L Lysine
% adher. cells
300
200
100
0
30´
60´
120´
time
P
NTC
#4
#8
b
Nomber of foci(A.U.)
200
100
0
15
30
120
180
time
Parental
NTC
#4
#8
BF
BC
P
NTC
#4
#8

Figure 6

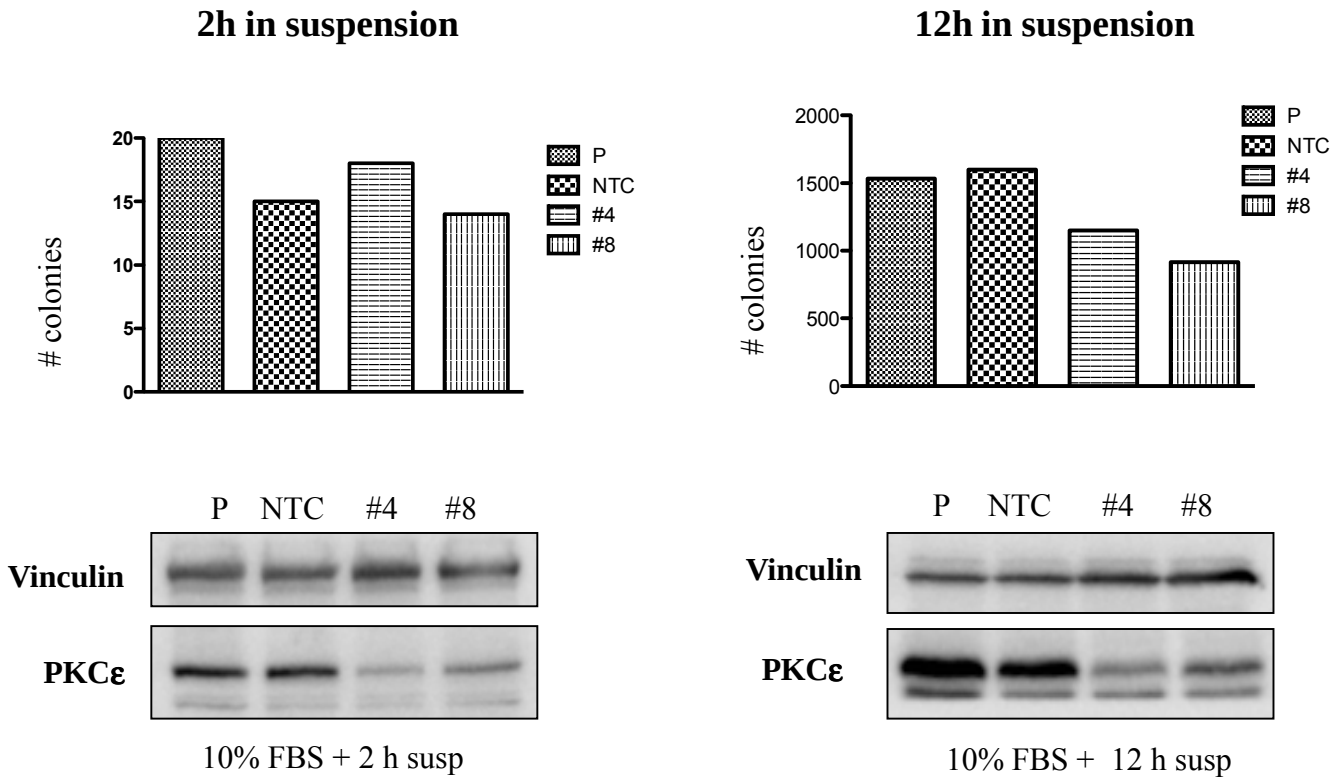
2h in suspension
12h in suspension
colonies
20
15
10
5
0
2000
1500
1000
500
0
P
NTC
#4
#8
P NTC #4 #8
Vinculin
PKCε
10% FBS + 2 h susp
10% FBS + 12 h susp

Figure 7

a

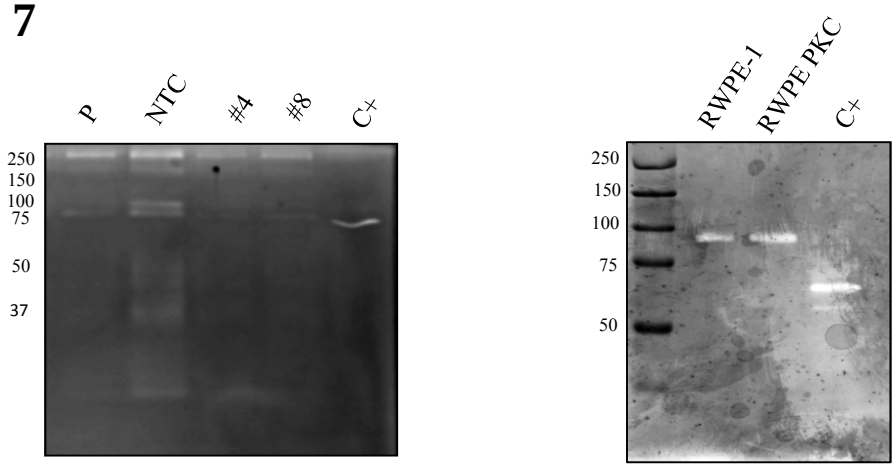

b

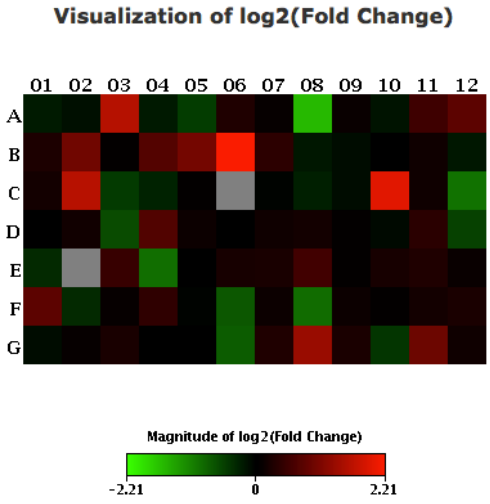

Layout	01	02	03	04	05	06	07	08	09	10	11	12
A	APC **-1.18** OKAY	BRMS1 **-1.10** OKAY	CCL7 **3.03** B	CD44 **-1.16** OKAY	CD82 **-1.43** OKAY	CDH1 **1.21** OKAY	CDH11 **1.06** OKAY	CDH6 **-3.07** A	CDKN2A **1.08** OKAY	CHD4 **-1.13** OKAY	COL4A2 **1.47** OKAY	CST7 **1.77** A
B	CTBP1 **1.20** OKAY	CTNNA1 **1.97** A	CTSK **1.03** OKAY	CTSL1 **1.65** OKAY	CXCL12 **2.04** B	CXCR2 **4.63** A	CXCR4 **1.32** OKAY	DENR **-1.16** OKAY	EPHB2 **-1.09** OKAY	ETV4 **-1.00** OKAY	EWSR1 **1.12** OKAY	FAT1 **-1.15** OKAY
C	FGFR4 **1.14** OKAY	FLT4 **3.07** B	FN1 **-1.42** OKAY	FXYD5 **-1.24** OKAY	GNRH1 **1.04** OKAY	HGF **-1.00** C	HPSE **-1.03** OKAY	HRAS **-1.21** OKAY	HTATIP2 **-1.09** OKAY	IGF1 **3.94** B	IL18 **1.10** OKAY	IL1B **-1.97** OKAY
D	ITGA7 **-1.00** OKAY	ITGB3 **1.13** OKAY	KISS1 **-1.58** OKAY	KISS1R **1.64** B	KRAS **1.09** OKAY	MCAM **1.01** OKAY	MDM2 **1.12** OKAY	MET **1.14** OKAY	METAP2 **1.04** OKAY	MGAT5 **-1.07** OKAY	MMP10 **1.30** OKAY	MMP11 **-1.48** OKAY
E	MMP13 **-1.28** OKAY	MMP2 **-1.00** C	MMP3 **1.40** A	MMP7 **-1.95** B	MMP9 **-1.00** OKAY	MTA1 **1.16** OKAY	MTSS1 **1.17** OKAY	MYC **1.48** OKAY	MYCL1 **1.02** OKAY	NF2 **1.15** OKAY	NME1 **1.21** OKAY	NME4 **1.08** OKAY
F	NR4A3 **1.77** OKAY	PLAUR **-1.29** OKAY	PNN **1.06** OKAY	PTEN **1.33** B	RB1 **-1.04** OKAY	RORB **-1.71** B	RPSA **1.09** OKAY	SERPINE1 **-1.91** OKAY	SET **1.09** OKAY	SMAD2 **1.02** OKAY	SMAD4 **1.14** OKAY	SRC **1.18** OKAY
G	SSTR2 **-1.09** OKAY	SYK **1.06** OKAY	TCF20 **1.16** OKAY	TGFB1 **1.01** OKAY	TIMP2 **1.01** OKAY	TIMP3 **-1.73** OKAY	TIMP4 **1.21** B	TNFSF10 **2.57** B	TP53 **1.18** OKAY	TRPM1 **-1.38** B	TSHR **1.95** B	VEGFA **1.10** OKAY

Figure 8

a

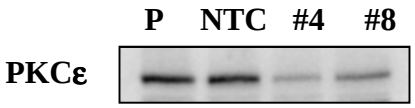

b

	Positive for metastasis	Number of micrometastasis
P	+	6
NTC	+	7
#4	-	-
#8	+	1

c

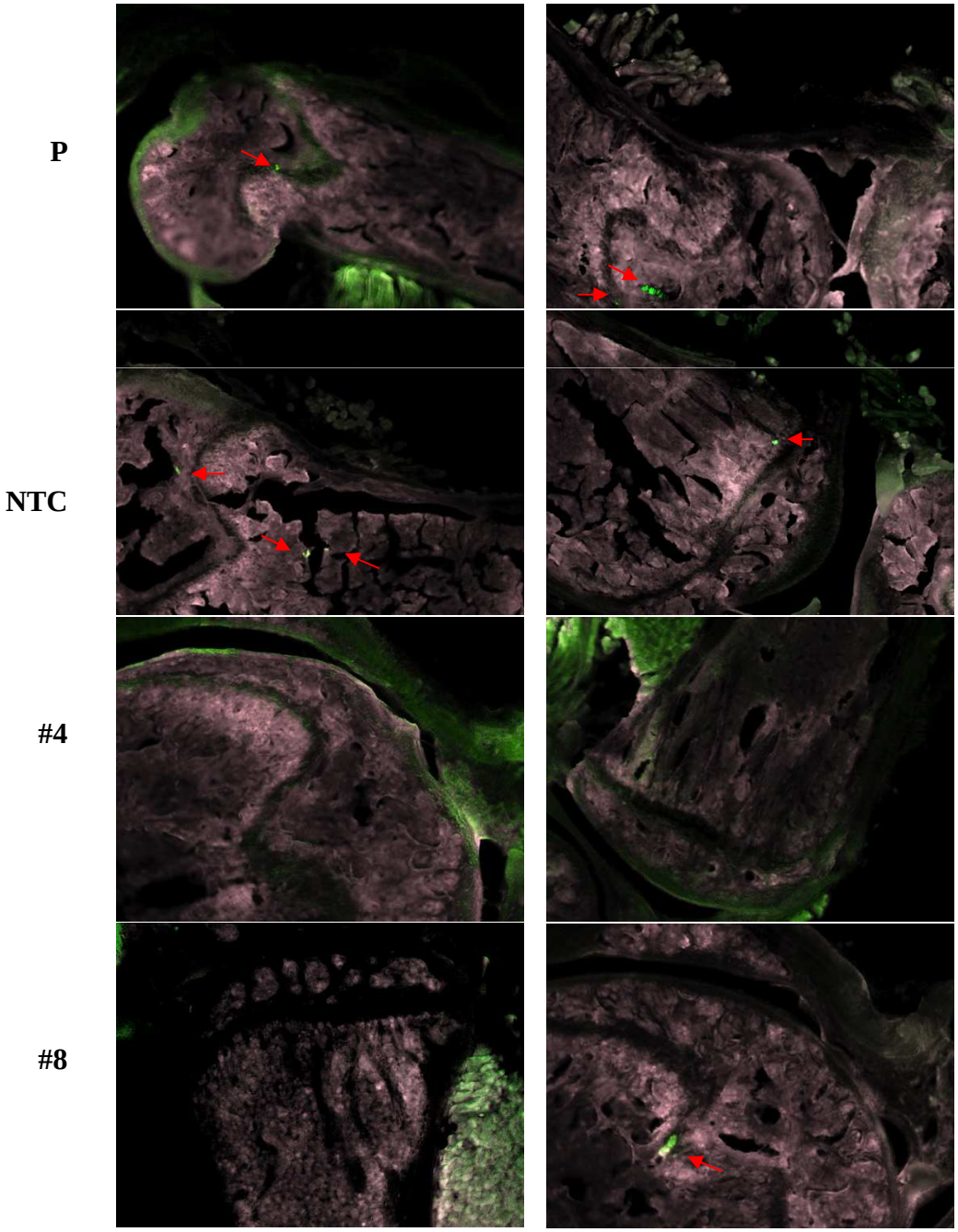

Figure 9

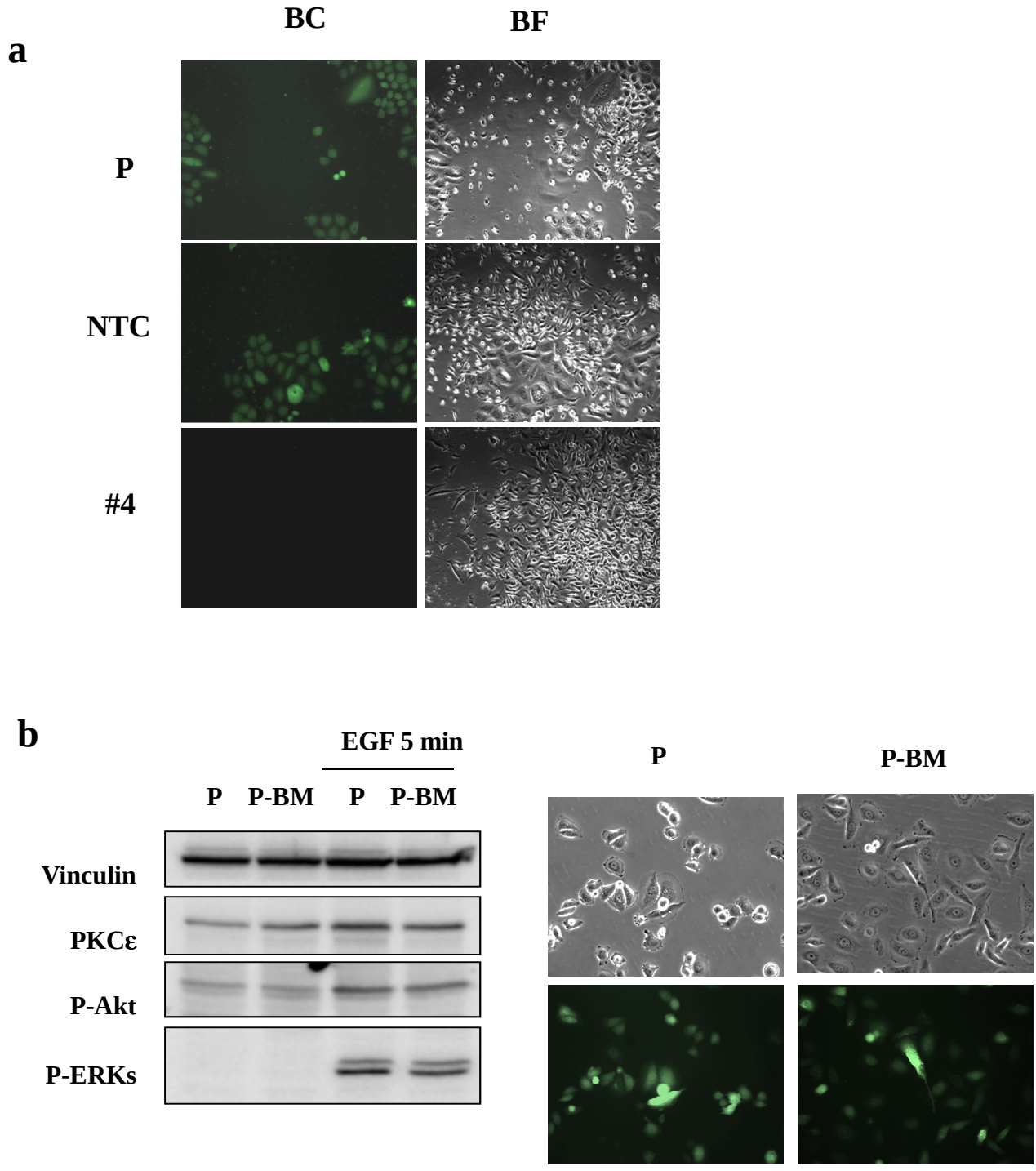
a
BC
BF
P
NTC
#4
b
EGF 5 min
P
P-BM
P
P-BM
Vinculin
PKCε
P-Akt
P-ERKs
P
P-BM

Figure 10

a

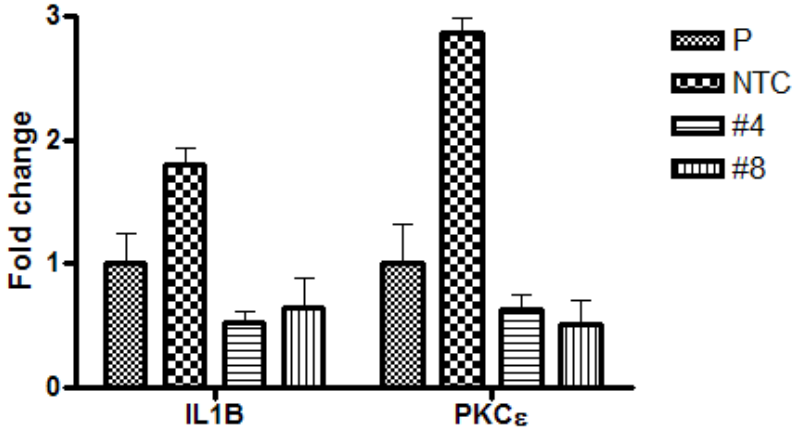
Fold change
3
2
1
0
IL1B
PKCε
P
NTC
#4
#8

b

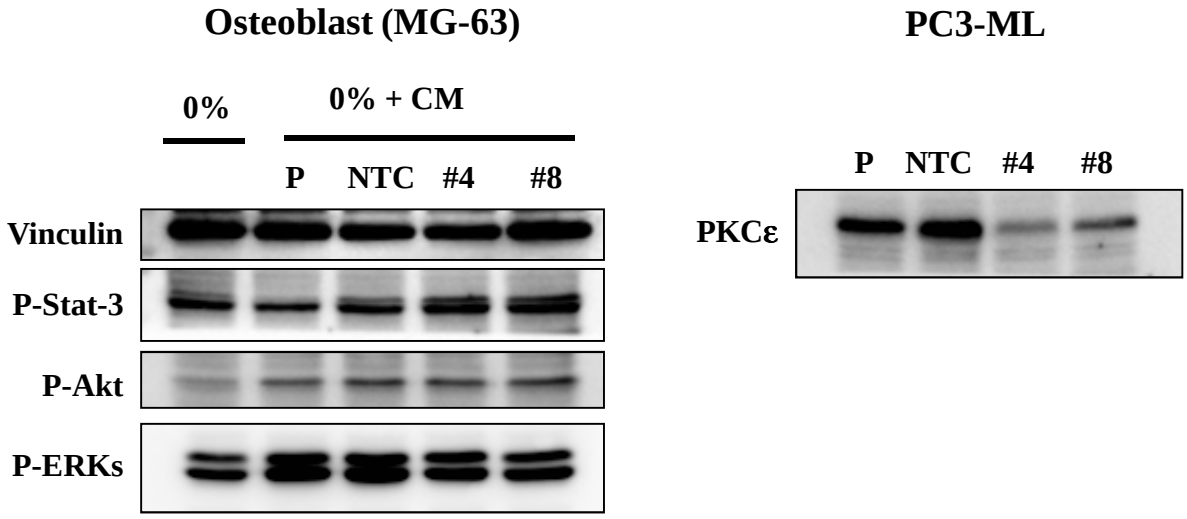
Osteoblast (MG-63)
PC3-ML
0%
0% + CM
P
NTC
#4
#8
Vinculin
P-Stat-3
P-Akt
P-ERKs
PKCε